3D Crack Skeleton Extraction from Mobile LiDAR Point Clouds

Yongtao Yu[1], Jonathan Li[1*,2], Haiyan Guan[2], and Cheng Wang[1]
[1]School of Information Science and Engineering, Xiamen University, Xiamen, Fujian 361005, China
[2]Department of Geography and Environmental Management, University of Waterloo, Waterloo, Ontario N2L 3G1, Canada
Email: allennessy.yu@gmail.com, *junli@uwaterloo.ca, h6guan@uwaterloo.ca, cwang@xmu.edu.cn

***Abstract* — This paper presents a novel algorithm for extracting 3D crack skeletons from 3D point clouds acquired by a mobile Light Detection and Ranging (LiDAR) system. This algorithm uses intensity information of cloud clouds to identify pavement cracks that usually exhibit lower intensities compared to their surroundings. First, crack candidates are extracted by applying the Otsu thresholding algorithm. Then, a spatial density filter is used to remove outliers. Next, crack points are grouped into crack-lines using a Euclidean distance clustering method. Finally, crack skeletons are extracted based on an L_1-medial skeleton extraction method. The proposed algorithm has been tested on a set of mobile LiDAR point clouds acquired by a state-of-the-art RIEGL VMX-450 mobile LiDAR system. The results demonstrate the efficiency and reliability of the proposed algorithm in extracting 3D crack skeletons.**

Index Terms – Crack skeleton, mobile LiDAR, point cloud, spatial density, L_1-median

I. INTRODUCTION

Rapid and cost-effective detection of road surface distress plays an important role in road surface maintenance. Pavement cracks, as the most common type of asphalt road surface distress, are usually caused by fracture due to excessive loading, fatigue, thermal changes, moisture damage, slippage, or contraction. Generally, according to the shape and position, cracks are classified into the following categories: fatigue, longitudinal, alligator, edge, reflection, block, and transverse [1], [2]. Detecting pavement cracks not only assists in maintaining and repairing road surface distress, but also provides an effective means to prevent potential disasters and improve traffic safety. Therefore, automated and cost-effective techniques for pavement crack detection are urgently in demand.

Crack detection has been intensively studied in literature. Most of existing methods for crack detection are basically based on images. A 3D crack detection method presented in [3] was based on a combination of an image-based 3D reconstruction method and a 3D crack detection algorithm. An integration model consisting of crack quantification, change detection, neural networks, and 3D visualization models was developed in [4] to retrieve concrete properties for bridge inspection. Similarly, an optimized eight-direction Sobel edge detector [5] was proposed to detect bridge cracks. The one-class Parzen density estimation and entropy reduction were used in [6] to detect pavement cracks. First, a one-class clustering method, using Parzen density estimation, was applied to select image areas likely to contain cracks. Next, the selected blocks were filtered using the UNITA entropy reduction properties and later automatically labeled as containing cracks or not. A novel algorithm was introduced in [7] for detecting cracks from underwater dam images. This algorithm used image intensities to generate a 3D spatial surface. The cracks that are difficult to describe in 2D images were regarded well as ditches in the 3D spatial surface. Then, by analyzing the characteristics of ditch space curvatures, a space detection method was used to obtain the ditch information, which was mapped to 2D surfaces as the cracks.

Light Detection and Ranging (LiDAR) technologies have developed rapidly in the past decades. The data acquired by LiDAR systems have also been used for a variety of applications, such as building reconstruction [8], tree modeling [9], DEM generation [10], and road feature extraction [11]. Among the LiDAR products, mobile LiDAR systems have become a promising means for basic surveying and mapping. Due to the properties of high-density, long-range, and cost-effective data acquisition, the point clouds acquired by mobile LiDAR systems have become an indispensable source for 3D city reconstruction and road feature extraction. The average density of the point clouds on the road surface can reach up to 4000 points/m^2 with a moving speed of 50 km/h; therefore, mobile LiDAR systems provide a promising way to detect pavement cracks.

In this paper, we propose a novel algorithm for extracting 3D crack skeletons directly from mobile LiDAR point clouds. Basically, mobile LiDAR systems use near-infrared radiations to measure objects' topologies and record the backscattered reflectance in a form of intensity. Therefore, first, we make use of the intensity information of the point clouds to identify crack candidates by applying the Otsu thresholding algorithm [12]. Then, a spatial density filter is developed to remove outliers in the identified crack candidates. Next, crack points are grouped into clusters representing individual crack-lines using a Euclidean distance clustering method. Finally, 3D crack skeletons are extracted by applying an L_1-medial skeleton extraction method [13]. The proposed algorithm has been tested on a set of 3D point clouds acquired by a state-of-the-art RIEGL VMX-450 mobile LiDAR system. The experimental results demonstrate the efficiency and reliability of the proposed algorithm in extracting 3D crack skeletons directly from mobile LiDAR point clouds.

II. METHOD

As shown in Fig. 1, the proposed algorithm for extracting 3D crack skeletons contains four steps: crack candidate identification, spatial density filtering, Euclidean distance clustering, and L_1-medial skeleton extraction.

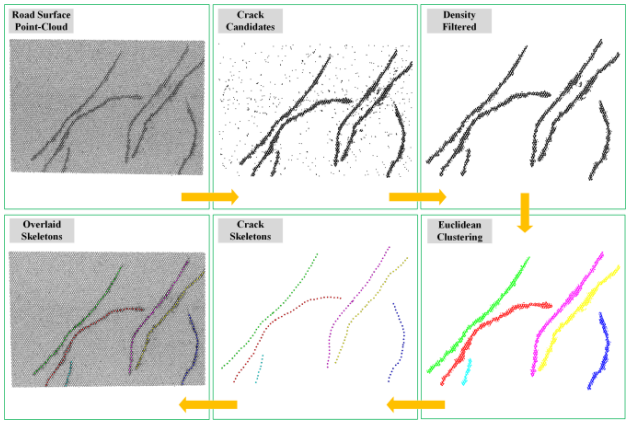

Fig. 1. Flowchart of the proposed 3D crack skeleton extraction algorithm.

A. Crack Candidate Identification

As shown in top left of Fig. 1, compared to the road surface, pavement cracks exhibit relatively lower intensities in the point cloud. However, due to the reflectance properties of laser beams and surface properties of the measured targets, the backscattered intensities vary greatly in the resultant point cloud. Therefore, to simplify the processing, first, we normalize the intensities of the data points in a point cloud into the range of [0,255] as follows:

$$G_i = 255 \times \frac{I_i - \min_{j=1}^{n} I_j}{\max_{j=1}^{n} I_j - \min_{j=1}^{n} I_j}, \quad (1)$$

where G_i denotes the normalized intensity of point i; I_i is the raw intensity of point i; n denotes the number of points in the point cloud.

Then, to extract the points belonging to pavement cracks from the road surface point cloud, we apply the Otsu thresholding algorithm [12] to identify crack candidates based on the normalized intensities. The Otsu thresholding algorithm determines a global optimal threshold that maximizes the ratio of between-class variance to the within-class invariance. After the threshold is calculated, the points with intensities below the threshold are regarded as crack candidates, while the others are treated as background points and further removed. A visual example of the obtained crack candidates is shown in top center of Fig. 1.

B. Spatial Density Filtering

Due to the mechanism of mobile LiDAR systems, the intensities reflected from an object also depend on the ranges from the scanner center and the incident angles of the laser beams. Therefore, the identified crack candidates contain considerable outliers (see top center of Fig. 1). Generally, compared to crack points, the outliers distribute dispersedly and irregularly. The spatial densities of the outliers are lower than those of crack points. Thus, to effectively remove these outliers, we propose a spatial density filter that calculates the spatial density of each crack candidate and removes the candidates whose spatial densities lie below a pre-defined threshold d_s. The spatial density of crack candidate p_i is defined as follows:

$$d_i = 1 + \sum_{p_j \in N(p_i)} \exp\left(-\frac{\|p_i - p_j\|^2}{(r_d / 2)^2} \right), \quad (2)$$

where $N(p_i)$ denotes the neighborhood of crack candidate p_i; r_d is the size of the neighborhood. After the spatial densities of crack candidates are calculated, the crack candidates with spatial densities below d_s are regarded as outliers and further filtered out. A visual example of the extracted crack points after spatial density filtering is shown in top right of Fig. 1.

C. Euclidean Distance Clustering

As shown in top right of Fig. 1, the crack points belonging to a specific crack-line are still isolated. In order to group the discrete crack points into clusters representing individual crack-lines, we adopt a Euclidean distance clustering method. The Euclidean distance clustering method utilizes the Euclidean distances between each pair of crack points to group them into separated clusters. Specifically, an unlabeled crack point is contained into a certain crack-line if and only if its shortest Euclidean distance to the crack points in this crack-line lies below a clustering threshold d_c. Otherwise, a new crack-line is created to contain this crack point. After Euclidean distance clustering, the discrete crack points are grouped to form separated crack-lines. Moreover, based on prior knowledge, the small-size clusters that are unlikely to be crack-lines are further removed. A visual example of the generated individual crack-lines is shown in bottom right of Fig. 1.

D. Crack Skeleton Extraction

L_1-median [14] has proved to be a simple and powerful statistical tool to compute the global center of a given set of points. In this paper, rather than computing a single global center, we apply the L_1-median locally to the crack-lines to generate a 3D skeleton representing the geometric structures of the crack-lines. Given a crack-line with a set of points $C = \{p_i\}_{i \in I}$, its associated skeleton $X = \{x_j\}_{j \in J}$ is calculated as follows [13]:

$$\arg\min_X \sum_{j \in J} \sum_{i \in I} \|x_j - p_i\| \exp\left(\frac{\|x_j - p_i\|^2}{(h/2)^2} \right) + R(X), \quad (3)$$

where h defines the local neighborhood size for the L_1-medial skeleton construction; I and J index the set of points in C and X, respectively; $R(X)$ is a repulsion term for regularizing the local distribution of X when a skeleton branch is locally formed.

To effectively construct the repulsion term in (3), as mentioned in [13], we adopt a weighted principal component analysis (PCA) method to detect skeleton branches. For each point x_j in X, we construct a covariance matrix for this point as follows:

$$C_j = \sum_{k \in J \setminus \{j\}} \exp\left(-\frac{\|x_k - x_j\|_2^2}{(h/2)^2} \right) (x_k - x_j)^T (x_k - x_j) \cdot \quad (4)$$

After eigenvalue decomposition on the covariance matrix, we obtain three eigenvalues λ_1^j, λ_2^j, and λ_3^j ($\lambda_1^j \geq \lambda_2^j \geq \lambda_3^j$) and the associated eigenvectors e_1^j, e_2^j, and e_3^j. Then, the directionality degree [13] of x_j within its local vicinity is defined as follows:

$$\delta(x_j) = \frac{\lambda_1^j}{\lambda_1^j + \lambda_2^j + \lambda_3^j} \cdot \quad (5)$$

Based on the directionality degree measure, the repulsion term in (3) is defined as follows:

$$R(X) = \sum_{j \in J} \eta_j \sum_{k \in J \setminus \{j\}} \frac{1}{\delta(x_j) \|x_j - x_k\|_2} \exp\left(-\frac{\|x_j - x_k\|_2^2}{(h/2)^2} \right), \quad (6)$$

where $\{\eta_j\}_{j \in J}$ are the balancing constraints among X [13]. The minimization of (3) can be effectively solved by an iterative contraction process [13].

After applying the L_1-median-based crack skeleton extraction method, the 3D crack skeleton of each crack-line is extracted. A visual example of the extracted 3D crack skeletons are shown in bottom center of Fig. 1.

III. Results and Conclusion

A. VMX-450 System and Point Cloud Data

The 3D point cloud data used in this study were acquired using a state-of-the-art RIEGL VMX-450 mobile LiDAR system (see Fig. 2) in Xiamen, China, which is a subtropical city located near the seaside. This system consists of two full-view RIEGL VQ-450 laser scanners, four high-resolution CCD cameras, and a set of inertial navigation systems (INS) including two global navigation satellite system (GNSS) antennas, an inertial measurement unit (IMU), and a wheel-mounted distance measurement indicator (DMI). The two laser scanners rotate to emit laser beams with a line scan speed of up to 400 scans per second and a maximum range of approximately 800 meters.

Caused by heavy moisture and transportation loads, there are many cracks on the road surface in this area. Due to a high measurement rate (about 1.1 million measurements per second) of the VMX-450 system, the point density near to the scanner center can reach up to 7000 points/m^2, and an average point density of more than 4000 points/m^2 can be obtained on the road surface. Therefore, these point cloud data provide promising data source for extracting pavement cracks for transportation-related applications. From the collected data, we selected several datasets for evaluating the performance of the 3D crack skeleton extraction algorithm.

Fig. 2. RIEGL VMX-450 mobile LiDAR system and its components.

B. Performance Assessment

As shown in Figs. 3(a), 4(a), and 5(a), we selected three road surface point clouds with different types of pavement cracks for evaluating our proposed algorithm. First, the Otsu thresholding algorithm was applied to threshold these road surface point clouds to identify crack candidates. Then, the spatial density filter with a local radius r_d = 0.1 m and a density threshold d_s = 6.0 was used to remove outliers (see Figs. 3(b), 4(b), and 5(b)). Next, the isolated crack points were grouped into individual crack-lines through the Euclidean distance clustering method with a clustering threshold d_c = 2.5 cm (see Figs. 3(c), 4(c), 5(c)). Finally, 3D crack skeletons were extracted using the L_1-medial skeleton extraction algorithm (see Figs. 3(d), 4(d), and 5(d)).

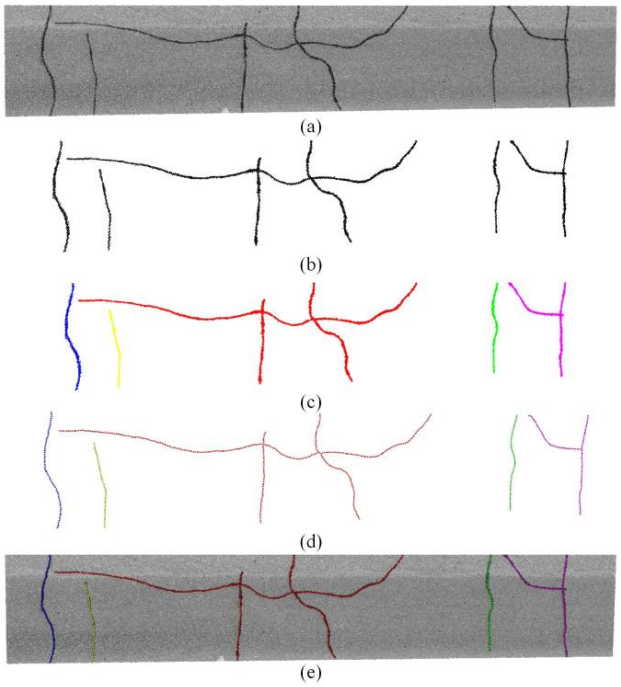

Fig. 3. (a) Road surface point cloud, (b) obtained crack points after spatial density filtering, (c) clustered individual crack-lines, (d) extracted 3D crack skeletons, and (e) overlaid result.

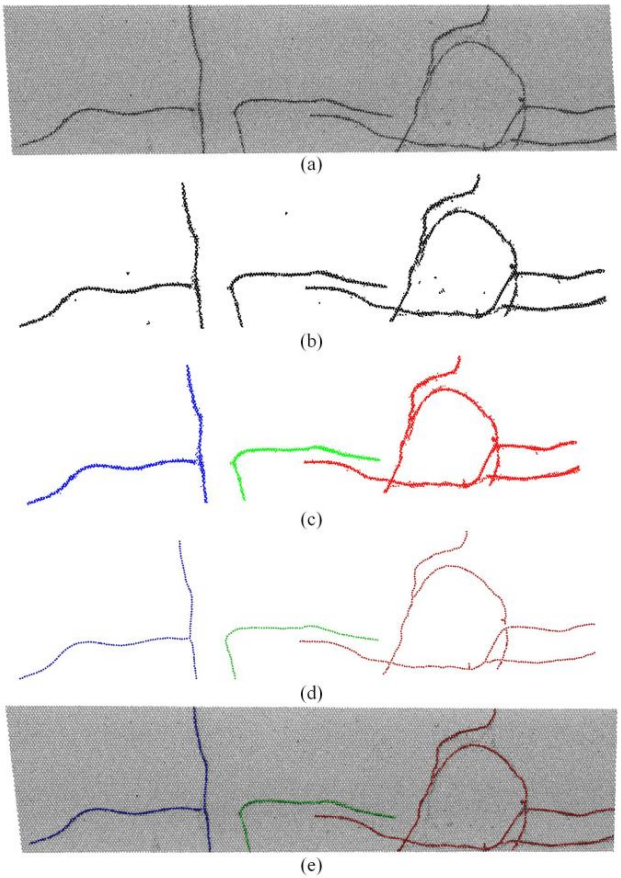

Fig. 4. (a) Road surface point cloud, (b) obtained crack points after spatial density filtering, (c) clustered individual crack-lines, (d) extracted 3D crack skeletons, and (e) overlaid result.

We also overlaid the extracted 3D crack skeletons onto the road surface point clouds for visual inspection, as shown in Figs. 3(e), 4(e), and 5(e), respectively. As seen from the overlaid results, we conclude that the proposed algorithm performs very well and achieves acceptable results. In addition, the proposed algorithm was implemented using C++ and executed very fast in extracting 3D crack skeletons. Therefore, we provide a promising and rapid framework for extracting 3D crack skeletons directly from 3D mobile LiDAR point clouds.

REFERENCES

[1] H. Lee, "Standardization of distress measurements for the network-level pavement management system, pavement management implementation," *ASTM STP 1121*, pp. 424-436, 1992.

[2] K. H. McGhee, "Automated pavement distress collection techniques," *National Cooperative Highway Research Program (NCHRP) Synthesis 334*, Washington, DC, 2004.

[3] M. M. Torok, M. Golparvar-Fard, and K. B. Kochersberger, "Image-based automated 3D crack detection for post-disaster building assessment," *Journal of Computing in Civil Engineering*, 2013.

[4] R. S. Adhikar, O. Moselhi, and A. Bagchi, "Image-based retrieval of concrete crack properties for bridge inspection," *Automation in Construction*, vol. 39, pp. 180-194, 2014.

[5] J. Lu, P. Song, and K. Han, "Improved imaging algorithm for bridge crack detection," in *Fourth International Conference on Digital Image Processing (ICDIP 2012)*, pp. 83340P-83340P, 2012.

[6] H. Oliveira, J. J. Ceiro, and P. L. Correia, "Improved road crack detection based on one-class Parzen density estimation and entropy reduction," in *Proc. 2010 IEEE 17th International Conference on Image Processing*, Hong Kong, pp. 2201-2204, 2010.

[7] C. Chen, J. Wang, L. Zou, J. Fu, and C. Ma, "A novel crack detection algorithm of underwater dam image," *2012 International Conference on Systems and Informatics*, pp. 1825-1828, 2012.

[8] P. Musialski, P. Wonka, D. G. Aliaga, M. Wimmer, L. van Gool, and W. Purgathofer, "A survey of urban reconstruction," *Computer Graphics Forum*, vol. 32, no. 6, pp. 146-177, 2013.

[9] Y. Livny, F. Yan, M. Olson, B. Chen, H. Zhang, and J. El-Sana, "Automatic reconstruction of tree skeletal structures from point clouds," *ACM Transactions on Graphics*, vol. 29, no. 6, pp. 151:1-8, 2010.

[10] C. Wang and N. F. Glenn, "Integrating LiDAR intensity and elevation data for terrain characterization in a forested area," *IEEE Geoscience and Remote Sensing Letters*, vol. 6, no. 3, pp. 463-466, 2009.

[11] S. Pu, M. Rutzinger, G. Vosselman, and S. O. Elberink, "Recognizing basic structures from mobile laser scanning data for road inventory studies," *ISPRS Journal of Photogrammetry and Remote Sensing*, vol. 66, no. 6, pp. S28-S39, 2011.

[12] N. Otsu, "A threshold selection method from gray-level histograms," *IEEE Transactions on Systems, Man, and Cybernetics*, vol. 9, no. 1, pp. 62-66, 1979.

[13] H. Huang, S. Wu, D. Cohen-Or, M. gong, H. Zhang, G. Li, and B. Chen, "L_1-medial skeleton of point cloud," *ACM Transactions on Graphics*, vol. 32, no. 4, pp. 65:1-8, 2013.

[14] C.G. Small, "A survey of multidimensional medians," *International Statistical Review*, vol. 58, no. 3, pp. 263-277, 1990.

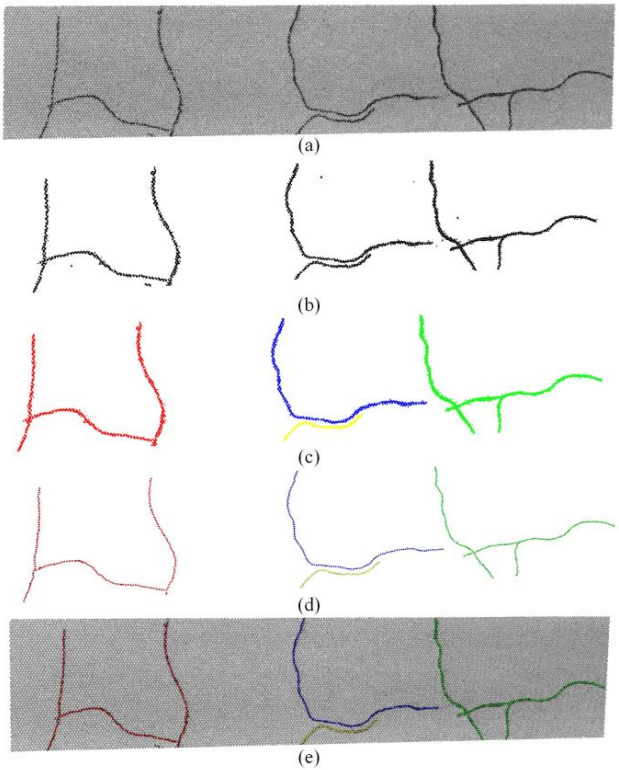

Fig. 5. (a) Road surface point cloud, (b) obtained crack points after spatial density filtering, (c) clustered individual crack-lines, (d) extracted 3D crack skeletons, and (e) overlaid result.